

The Galactic Center as a Paradigm for Low Luminosity Nuclei?

What can be learned from SgrA* for the central engine and conditions of star formation in nuclei of Seyfert galaxies and low luminosity nearby QSOs

The K-band identification of the DSO/G2 source from VLT and Keck data

Andreas Eckart*

E-mail: eckart@ph1.uni-koeln.de

**S. Britzen², M. Horrobin¹, M. Zamaninasab², K. Mužić³, N. Sabha^{1,2},
B. Shahzamanian^{1,2}, S. Yazici¹, L. Moser¹, J. Zuther¹, M. Garcia-Marin¹,
M. Valencia-S.¹, M. Bursa⁴, G. Karssen¹, V. Karas⁴, B. Jalali¹, M. Vitale^{2,1},
M. Bremer¹, S. Fischer¹, S. Smajic¹, C. Rauch², D. Kunneriath⁴, J. Moutaka^{5,6},
C. Straubmeier¹, Y.E., Rashed¹, C. Iserlohe¹, G. Busch¹, K. Markakis^{2,1},
A. Borkar^{2,1}, A. Zensus^{2,1}**

1) *I. Physikalisches Institut, Universität zu Köln, Zùlpicher Str. 77, 50937 Köln, Germany*

2) *Max-Planck-Institut für Radioastronomie, Auf dem Hügel 69, 53121 Bonn, Germany*

3) *European Southern Observatory, Alonso de Cordova 3107, Vitacura, Casilla 19, Santiago, 19001, Chile*

4) *Astronomical Institute, Academy of Sciences, Bocni II 1401, CZ-141 31 Prague, Czech Republic*

5) *Université de Toulouse; UPS-OMP; IRAP; Toulouse, France*

6) *CNRS; IRAP; 14, avenue Edouard Belin, F-31400 Toulouse, France*

The super-massive 4 million solar mass black hole (SMBH) SgrA* shows flare emission from the millimeter to the X-ray domain. The nucleus of the Milky Way has properties (stellar cluster, young stars, molecular gas and an accreting SMBH) that resemble those of currently higher luminous Low Luminosity Active Galactic Nuclei. A detailed analysis of the infrared light curves shows that the flares are probably generated in a single-state process forming a power-law distribution of the flux density. Near-infrared polarimetry shows signatures of strong gravity that are statistically significant against randomly polarized red noise. Details of the emission mechanism are discussed in a synchrotron/self-Compton model. SgrA* also allows to study the interaction of the SMBH with the immediate interstellar and gaseous environment of the central stellar cluster. Through infrared imaging of the central few arcseconds it is possible to study both inflow and outflow phenomena linked to the SgrA* black hole. In this context we also discuss the newly found dusty object that approaches SgrA* and present a comparison between recent Keck and VLT K-band data that clearly supports its detection as a $\sim 19^m$ K'-band continuum source.

*Nuclei of Seyfert galaxies and QSOs - Central engine & conditions of star formation ,
November 6-8, 2012*

Max-Planck-Institut für Radioastronomie (MPIfR), Bonn, Germany

*Speaker.

1. Introduction

Sagittarius A* (SgrA*) at the center of our galaxy is a highly variable near-infrared (NIR) and X-ray source which is associated with a $4 \times 10^6 M_{\odot}$ central SMBH. Zamaninasab et al. (2010, 2011) has shown that the polarized NIR flares exhibit patterns of strong gravity, as expected from in-spiraling material very close to the black hole's horizon. Therefore, it is mainly the strong flux variability that gives us certainty that we study the immediate vicinity of a SMBH and investigate the largely unknown flare processes. For bright high signal to noise flares, relativistic modeling of NIR polarization data and SED modeling of the multi-wavelength data can discriminate between pure Synchrotron and Self-Compton models (e.g. Eckart et al. 2012).

Given the unambiguous traces of recent activity of the Galactic Center it is worthwhile to compare its properties with those of currently even more active sources such as the class of low Low Luminosity Active Galactic Nuclei (LLAGN). A detailed comparison to the center of the Milky Way and an in-depth discussion of the LLAGNs as a source class has been given by Contini (2011) and Ho (2008). Contini (2011) finds that, based on radio as well as far-infrared continuum and line emission ([OI] $63\mu\text{m}$ & $145\mu\text{m}$, [NII] $122\mu\text{m}$, [CII] $158\mu\text{m}$), the physical properties of the Galactic Center compare well to properties found for faint LLAGN. Ho (2008) outlines that due to the short duty cycle of the Black Hole accretion, most AGN spend their life in a low state, such that the bulk of the population has relatively modest luminosities. He concludes that the absolute luminosity can no longer be used as a defining metric of nuclear activity, and a broader range of alternative mechanisms needs to be considered to explain the nature of LLAGNs. Although a comparison of radio to X-ray continuum spectra of the Galactic Center to those of some bona fide LLAGNs (like NGC 3147, NGC 4579, NGC 4203, NGC 4168, NGC 4235, and NGC 4450) shows remarkable similarities, the detailed e.g. radio properties of extreme low luminosity objects (like the GC) may be different from those of higher luminosity sources (e.g. Zuther et al. 2012, 2008). Observational constraints and theoretical models suggest that the LLAGN are linked to radiation inefficient accretion flows (RIAF) with luminosities of $10^{-7} L_{Edd}$ or less, and that at $L_{bol}/L_{Edd} \leq 10^{-3}$ the BLR disappears and a truncated or only temporarily existing disk is very likely (Laor 2003, Nicastro 2000, Xu & Cao 2007). In Fig.1 we summarize these findings in a model of a LLAGN in its 'off'- and 'on'-state. A more detailed understanding of LLAGN through a comparison to the Galactic Center will also be fruitful for the investigations of the fueling of central black holes and nuclear star formation on more luminous nearby AGN (e.g. Smajić et al. 2012, Fischer et al. 2012, Bremer et al. 2012, Valencia-S. et al. 2012, Scharwächter et al. 2011, Vitale et al. 2012).

2. Building Blocks of a Nucleus

Based on the findings presented by Contini (2011) and Ho (2008), the Galactic Center is ideally suited to study the building blocks (see sections 2.1 to 2.6) that are required to explain the thermal and non-thermal activities in a LLAGN. Given the correlation between the black hole mass and the stellar velocity dispersion in the bulge (which apparently largely holds independently on the possible presence a pseudo-bulge; Beifiori et al. 2012) and the fact that LLAGN are found in a large fraction of all massive galaxies (Maoz 2008), we can take the properties of the Galactic

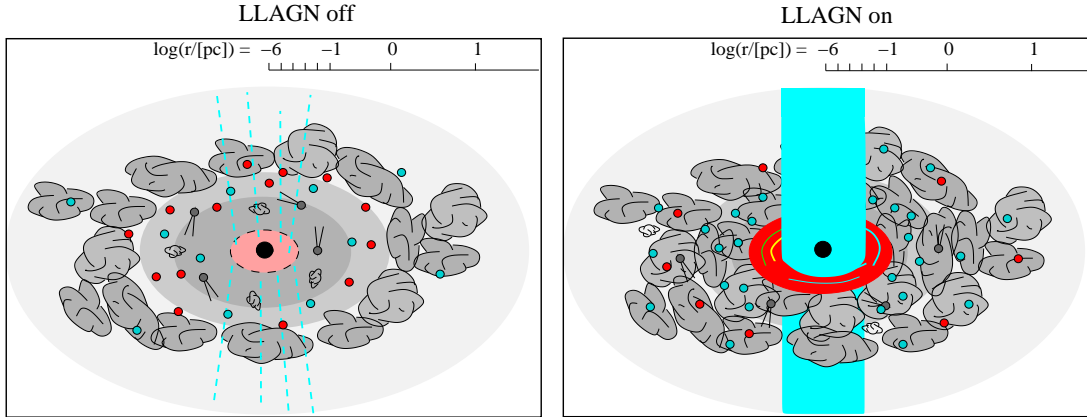


Figure 1: Inclined view on an LLAGN in its 'off' and 'on' state. A logarithmic scale along the semi-major axis is given. The molecular and atomic gas reservoir is indicated by dark clouds. The stellar cusp is indicated by the grey background. A temporary or truncated disk and a more substantial accretion disk are depicted by the pink and red disks surrounding the central black hole. The cyan lines and tube-like structure represent the not necessarily collimated wind or outflow off-state and a possible jet in the on-state. Red giants and blue young stars are shown as filled red and blue circles. In the off state the activity is dominated by rare and sporadic accretion events linked to dusty DSO-like objects (grey circles with commentary tails) and to smaller cloudlets that are clearly visible in the off-state image (see sections 2.3, 2.4 & 2.6 and Gillessen 2012, Eckart et al. 2013).

Center stellar cluster as a paradigm for bulges hosting the LLAGN. On size scales of the nuclear bulge the efficiency with which stars are formed from molecular gas appears to be dependent on the bulge properties (Fisher et al. 2013). However, the non-thermal AGN activity does not appear to be strongly linked to the amount of molecular gas available within the overall bulge (e.g. Krips et al. 2011, Bertram et al. 2007, Garcia-Burillo et al. 2008). Based on the NUGA sample of nearby AGN, Garcia-Burillo & Combes (2012; see also Casasola et al. 2010, 2011) show that secular evolution and dynamical decoupling of molecular gas structures are more likely the key ingredients to understand the AGN fueling and hence the overall AGN activity. Therefore, we speculate that also the star formation properties in the immediate vicinity ($< a$ few parsec) of the SMBH will depend on these factors rather than on more global bulge properties. This makes the Galactic Center an ideal case to study the conditions and impact of star formation in the immediate nuclear region.

2.1 The Stellar Cluster

The investigation of stellar properties of the Galactic Center (proper motions, radial velocities, colors, spectra, and variability) gives a clear view on the structure, dynamics, and stellar populations of the central cluster. First infrared stellar proper motion measurements were described by Eckart & Genzel (1996, 1997). Eckart et al. (2002) showed that the star S2 is in fact on a bound orbit and gave first orbital elements. More detailed elements of S2 and other stars were then successfully published by Schödel et al. (2002, 2003) and Ghez et al. (2003). Further improved orbital elements and derivations of the distance to the center from stellar orbits and proper motions were

given by Eisenhauer et al. (2005) and Gillessen et al. (2009). Schödel, Merritt & Eckart (2009) measured the proper motions of more than 6000 stars within the central stellar cluster (see also Schödel et al. 2010). These stars are within about 1.0 pc of SgrA*. They find that the bulk of the cluster rotates parallel to the Galactic rotation, while the velocity dispersion σ appears isotropic (see details in their paper). A Keplerian fall-off of σ due to the central point mass is detectable at separations of only a few 0.1 pc from SgrA* (see also Sabha et al. 2012). The authors find a best-fit black hole mass of $3.6 \pm (0.2-0.4) \times 10^6 M_{\odot}$ which is consistent with the mass inferred from the orbits of the individual S-cluster stars close to SgrA*. Hence, in terms of the SMBH mass the Galactic Center may be taken as a representative case for other nuclei, since comparable or even lower black hole masses are also indicated in other AGN (e.g. Valencia-S. et al. 2012).

2.2 The conditions for Star Formation

The polarization of stars measured at NIR wavelengths (Witzel et al. 2011; Buchholz et al. 2011, 2013, Rauch et al. 2013) allows us to separate objects that are polarized due to their local or intrinsic dust distributions from those that are polarized (predominantly only) due to the Galactic foreground. The detailed near- and mid-infrared properties of these dusty objects are outlined in several papers (Rauch et al. 2013, Eckart et al. 2013, Moutaka et al. 2009, Moutaka et al. 2004, Viehmann et al. 2006, 2005). The Galactic Center stellar cluster contains several young luminous He-stars that arrange themselves in at least one disk, indicating that they have been formed recently (Do et al. 2009, 2003, Eisenhauer et al. 2005, Levin & Beloborodov, 2003, and references there in). The IRS13N complex (Eckart et al. 2004, Muzic et al. 2008) consists of a group of infrared excess sources located just north of IRS13E. Together with the cometary shaped objects X3 and X7 (Muzic et al. 2010) and the G2/DSO (Gillessen 2012, Eckart et al. 2013), these are clear indications for the presence of dust enshrouded objects and ongoing star formation in the central stellar cluster. The Galactic Center can therefore serve as a laboratory where the conditions for star formation in a dense nuclear stellar cluster can be studied in detail.

2.3 The Dusty S-cluster Object

Recently, Gillessen et al. (2012, 2013) reported a fast moving infrared excess source (G2) which they interpret as a core-less gas and dust cloud approaching SgrA* on an elliptical orbit. Eckart et al. (2013) present first K_s -band identifications and proper motions of this dusty S-cluster object (DSO). In 2002-2007 it is confused with star S63, but free of confusion again since 2007. Its NIR colors and a comparison to other sources in the field imply that it could rather be an IR excess star than a core-less gas and dust cloud (Eckart et al. 2013). At a temperature of 450 K a pure dust contribution is very unlikely (Fig.15 in Eckart et al. 2013). Also we find very compact L' -band emission ($<0.1''$) contrasted by the extended ($\sim 0.2''$) $\text{Br}\gamma$ emission reported by Gillessen et al. (2012, 2013) and modeled by Schartmann et al. (2012) and Burkert et al. (2012). The presence of a star will change the expected accretion phenomena, since a stellar Roche lobe may retain much of the material (Eckart et al. 2013) during and after the peri-bothron passage.

From Fig.2 we can see that in 2004 there was a $8.6\mu\text{m}$ source component at the position of the DSO in 2004 or the position of the DSO/G2 'tail' in 2012 (Gillessen et al. 2012, 2013). Extended flux density at that location was already indicated in the MIR continuum map presented by Stolovy et al. (1996). Given the $8.6\mu\text{m}$ dust emission at the current 'tail' position (Fig.2) and the large

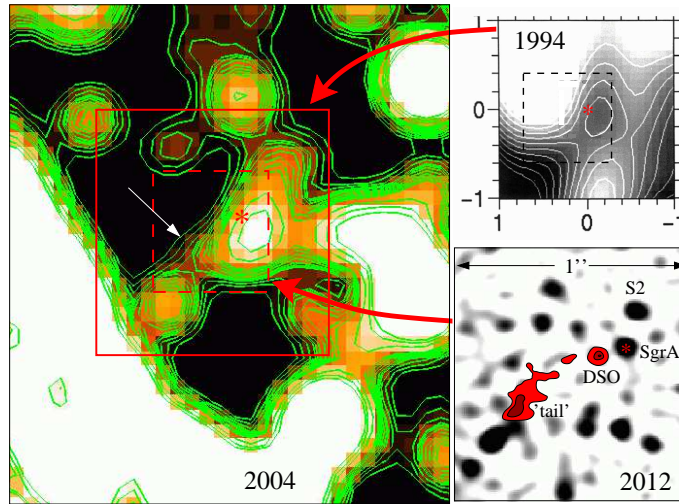


Figure 2: The 2004 VISIR and 1994 Palomar (Stolovy et al. 1996) 8.6 micron images, a source/flux ridge at the position of the DSO/G2 'tail' can be identified (white arrow). A 2012 NACO Ks-band image with the DSO 'tail' contours in red is shown. The image scales are given in arcsecond.

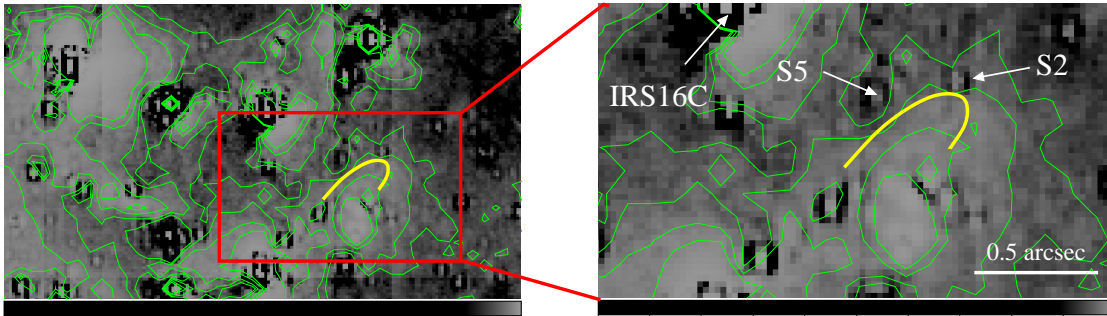


Figure 3: The Bry line emission (grey scale and contours) towards the central few arcseconds as obtained from narrow band filter observations with NACO (Kunneriath et al. 2012). The positions of some stars are labeled in the continuum subtracted image. We also show the approximate orbit of the DSO from 2002 to beyond 2013 (Eckart et al. 2013). The entire region is highly confused in its Bry line emission.

amount of confusion emission in the central region (Fig.3) this suggests another interpretation: The DSO/G2 'tail' seen in recent years is in fact a background component, possibly within the mini-spiral gas/dust flow. This is supported by the very low radial velocity and proper motion of the extended 'tail' component (Fig.7 in Gillessen et al. 2013 and Fig.10 in Schartmann et al. 2012). If the 'tail' component is indeed a background source that is not associated to the fast moving dusty object, then the DSO may be a compact source comparable to the cometary shape sources X3 and X7 (Muzic et al. 2010). Its smaller size compared to X3 and X7 can be explained by the higher particle density within the accretion stream close to SgrA* (e.g. Shcherbakov & Baganoff 2010). Its size also depends on how possible earlier passages close to SgrA* influence the distribution of gas and dust close to a possible star at the center of the DSO. The long dust lane feature that crosses

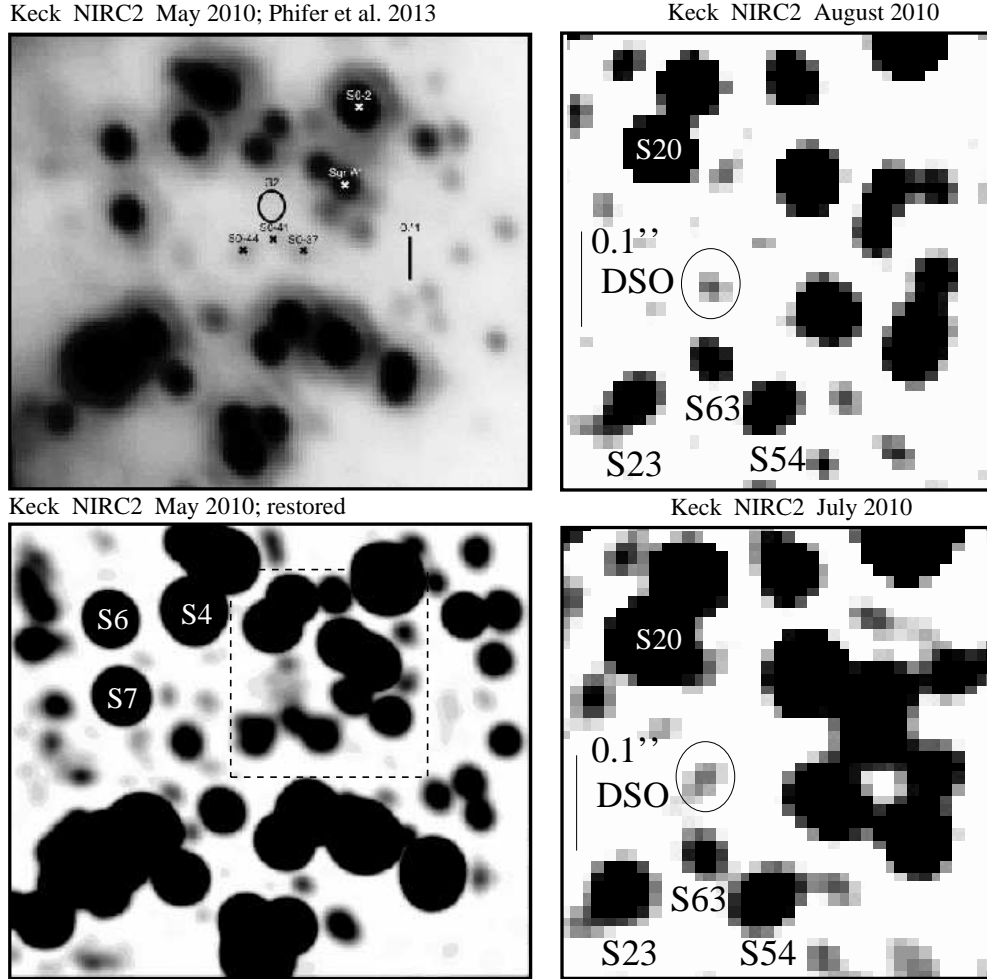


Figure 4: Comparison between Fig.2c by Phifer et al. (2013) (top left) and the restored version (bottom left) showing fainter structure in the same image that corresponds surprisingly well to structure reported by Eckart et al. (2013) in Fig.A.1. The public 2010 August 2010 (top right) and July (bottom right) Keck data reduced. The DSO can clearly be identified close to the center of the 3σ contour of the Br γ line emission reported by Phifer et al. (2013). This contour line is also shown as a black ellipse in the panels on the right side. The dashed rectangle in the bottom left image depicts the area of the image sections shown on the right.

the mini-spiral to the south-east of the DSO (Fig.7 in Gillessen et al. 2013) may then simply be a consequence of the interaction between the two rotation gas disk components that are associated with the northern arm and the eastern arm (Fig.21 in Zhao et al. 2009, and Fig.10 in Vollmer & Duschl 2000). If upcoming observations can confirm that the 'tail' component is not associated with the DSO, it does not need to be taken into account by future simulations. New simulations are needed that include the presence of a star and go beyond the assumption of a pure gas/dust cloud.

2.4 Confirmation of the K-band continuum detection of the DSO through Keck data

Given that the role of the DSO is important in the context of nuclear stellar populations and

date	decimal date	integration time (sec)	R.A. offset arcsec	DEC. offset arcsec
2008 05 20	2008.38	140	0.179	-0.062
2009 05 02	2009.33	616	0.170	-0.051
2010 07 05/06	2010.52	4760	0.151	-0.039
2010 08 14/15	2010.62	4760	0.144	-0.042
2011 07 18	2011.55	5236	0.117	-0.023

Table 1: List of public Keck data used for the present analysis and positions of the K'-band identification of the DSO based on this data. From their scattering we estimate the uncertainties of the R.A. and DEC. offsets to be of the same order as the value of 14 mas given by Eckart et al. (2013).

that its physical structure is essential for predictions and interpretations of the expected interaction with SgrA*, a comparison to additional observational data at $2\mu\text{m}$ wavelength is useful. Recently, Phifer et al. (2013) stated that, based on Keck data, they cannot detect the DSO in K'-band down to a limit of $K=20$. In a K'-band image they show an empty aperture at the position of the Br γ emission of the DSO. Size and shape of the aperture are given by the 3σ contour line of the Br γ line emission. Indeed, a simple visual inspection of this aperture in Fig.2c in Phifer et al. (2013) shows no source fainter than about 18.5 magnitude. We took Fig.2c by Phifer et al. (2013), removed all labels within the image by interpolation and reestablished a linear flux density scale using known source fluxes from the corresponding VLT data. The result is shown in Fig.4. It reveals a structure surprisingly similar to what Eckart et al. (2013) show for 2010 and we can clearly identify flux density at the position of the DSO counterpart at K'-band.

In order to further confirm the presence of the DSO at $2\mu\text{m}$ wavelength we reduced all publicly available K'-band imaging data obtained by the Keck that contain the SgrA* region. The results for epochs 2008, 2009, 2010, and 2011 are shown in Fig.5 and listed in Tab. 1. In order to fully exploit the data, we applied a Lucy deconvolution algorithm using the brightest source (IRS16SW) in the frame as a PSF reference. Inspection of other sources (e.g. IRS16C) in the field shows that the PSF structure at the location of the Airy ring changes on the 2% level as a function of position. In addition to a limited size PSF and a residual background this results in brightness dependant differential artifacts after deconvolution in the immediate surroundings of bright sources S4, S6, and S7. In the right panels of Fig.4 we show the DSO in a region that is sufficiently far away from bright stars and is therefore not heavily affected by this effect at the given sensitivity.

Based on the 2011 and 2012 Keck and NACO data we improved our kinematic model for stars S23, S63, S54, and S57, such that their position is now better represented in the crowded region 100mas to 150mas south of SgrA*. For this we changed the model parameters listed in Tab.6 by Eckart et al. (2013) by less than 3 times the 1σ uncertainty listed in the caption of that table. The improved parameters are listed here in Tab. 2. We show the results for epoch 2011 and 2012 for the NACO data in comparison with the new kinematic model in Fig. 6.

For the Keck data shown in Figs. 4 and 5 we find at all epochs very similar structures compared to those derived from the VLT data presented by Eckart et al. (2013). Based on the comparison

to VLT NACO L'- and K_s-band data (Eckart et al. 2013, Gillessen et al. 2013) we can clearly identify the DSO in its K'-band continuum emission as measured by the NIRC2 camera at the Keck telescope. Using the relative astrometric reference base on the positions of SgrA*, S2 as well as the positions of sources S23, S63, S54 (alias S0-44, S0-41, S0-37 in Keck nomenclature) as derived from their modeled projected orbits (Eckart et al. 2013) we can include the Keck results in the plots showing the DSO's right ascension and declination as a function of time. A comparison between the L'-band and K-band Br γ fits to the DSO trajectory published by Gillessen et al. (2013) and Phifer et al. (2013) as well as our K_s-band NACO (Eckart et al. 2013) and K'-band Keck identifications of the DSO is shown in Fig.7.

The comparison demonstrates that within the uncertainty of 14 mas (Eckart et al. 2013, Fig.A6) our DSO identification is in good agreement with the L'- and K_s-band results by Gillessen et al. (2013) and Eckart et al. (2013) as well as the K-band Br γ line emission results by Phifer et al. (2013). With respect to the VLT L'- and K_s-band results, the L'-band graph presented by Phifer et al. (2013) is systematically off by about 20 to 25 mas to the east and south. The comparison of the Keck and VLT results shows that there is a clear identification of the DSO in the K'-band continuum. Despite the admirably small formal errors in positions and orbital fits, the results appear to be affected by systematic effects. Our estimate of the uncertainties of 14 mas apparently represents the current systematic and statistical uncertainties quite well. This indicates that the combined L- and K-band results from both telescopes do currently not allow a very precise prediction of the DSO periapse.

Of course positions and flux densities for faint sources will not be as exact as for the bright members of the S-star cluster. The investigation of faint states of SgrA* by Witzel et al. (2013) showed that the flux density information towards low fluxes becomes increasingly unreliable. Sabha et al. (2012) showed that the flux densities and positions of faint sources will be influenced by the grainy and time variable distribution of faint cluster members in the background. Hence, one cannot expect that the information on flux density and position of the DSO is as accurate as it may possibly be for the brighter S-cluster sources.

2.5 Molecular Gas and Dust

A recent LABOCA sub-mm map of the thermal GC emission surrounding SgrA* is given by Garcia-Marin et al. (2011). They find that the innermost tens of parsecs of our Galaxy are characterized by the presence of molecular cloud complexes surrounding SgrA*. Using sub-mm maps, they describe the complex morphology of the molecular clouds and the circum-nuclear disk, along with their masses (of order 10^5 to $10^6 M_{\odot}$), and derive also the temperature and spectral index maps of the regions under study. The authors conclude that the average temperature of the dust is 14 ± 4 K. The spectral index map shows that the sub-mm emission of the 20 and 50 km/s clouds is dominated by dust emission. Comparatively, in the CND and its surroundings the spectral indices decrease toward SgrA* and has values between about 1 and -0.6. These numbers are mostly explained by a combination of dust, synchrotron, and free-free emission (in different proportions) at different positions. The presence of non-thermal emission also accounts for the apparent low temperatures derived in these very central regions. This indicates that obtaining dust temperatures in this region is difficult and possibly misleading. Requena-Torres et al. (2012) report sub-mm and millimeter spectroscopy measurements obtained with SOFIA/GREAT, Herschel/HIFI, and ground-

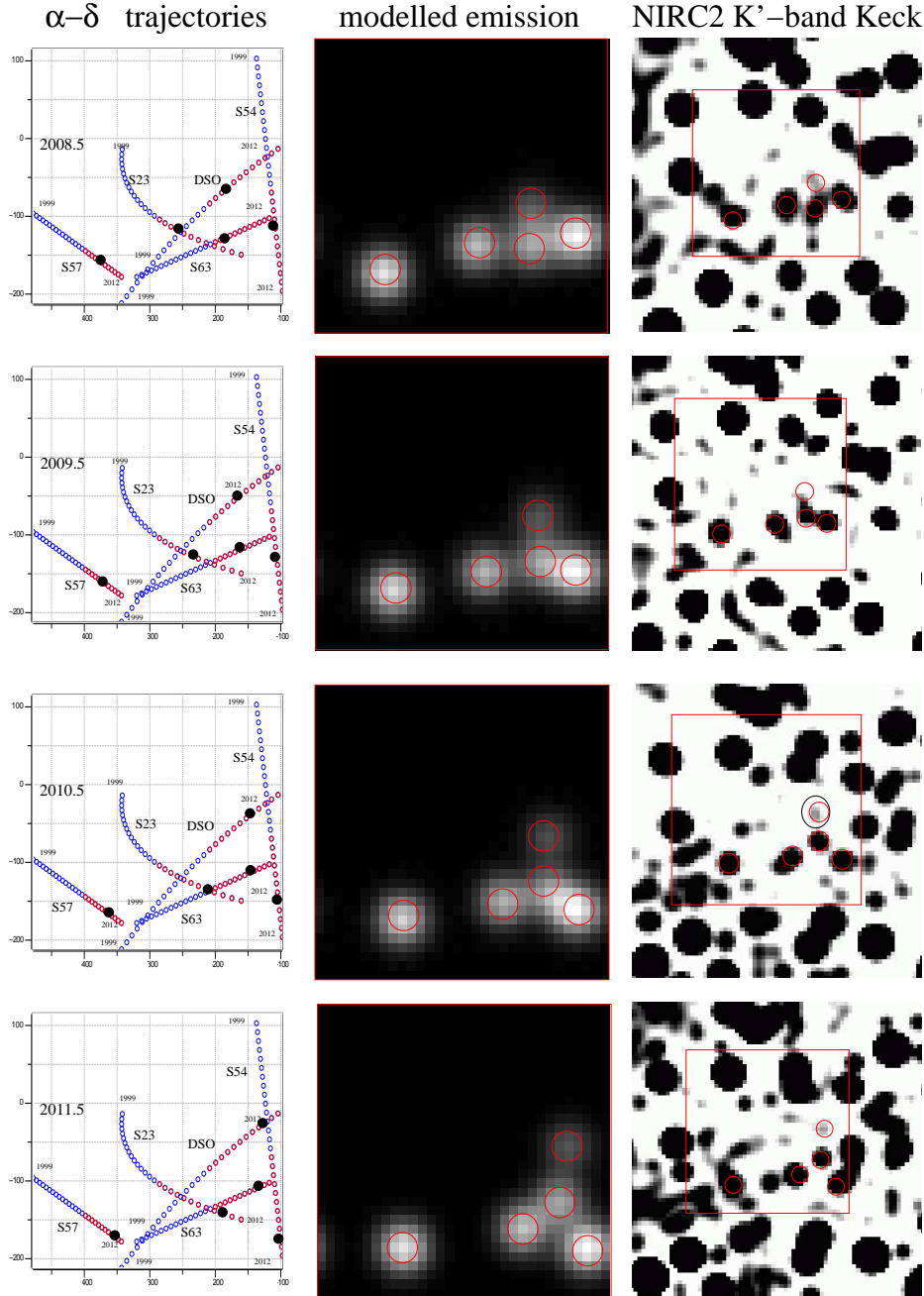


Figure 5: K'-band identification of the DSO using archival Keck NIRC2 data for epochs 2008 till 2011 and using the improved kinematic model from Tab 2. We show the relative positions of the stars S23, S57, S54, S63 and the DSO over the years 2008 - 2011 in comparison with K'-band Lucy-deconvolved Keck NIRC2 images (at $\sim 40\text{mas}$ resolution). We show the results of the model calculation (left) with the location of the sources on their sky-projected track (dot interval 0.5 years; 1999-2006.5 in blue, 2007-2012 in red), an image of the model with the sources indicated by red circles (middle; image size is $380\text{mas} \times 380\text{mas}$), and a deconvolved K'-band image with the modeled image section overlaid (right). For all years a source can clearly be identified at the L'-band position of the DSO. In 2008 it emerges from the confusion with S63 and shows up between the stars S23, S63, and S54 (alias S0-44, S0-41, S0-37 in Keck nomenclature) just north of S63. For 2010 we also show as a black ellipse the Br γ 3σ contour for the DSO given by Phifer et al. (2013).

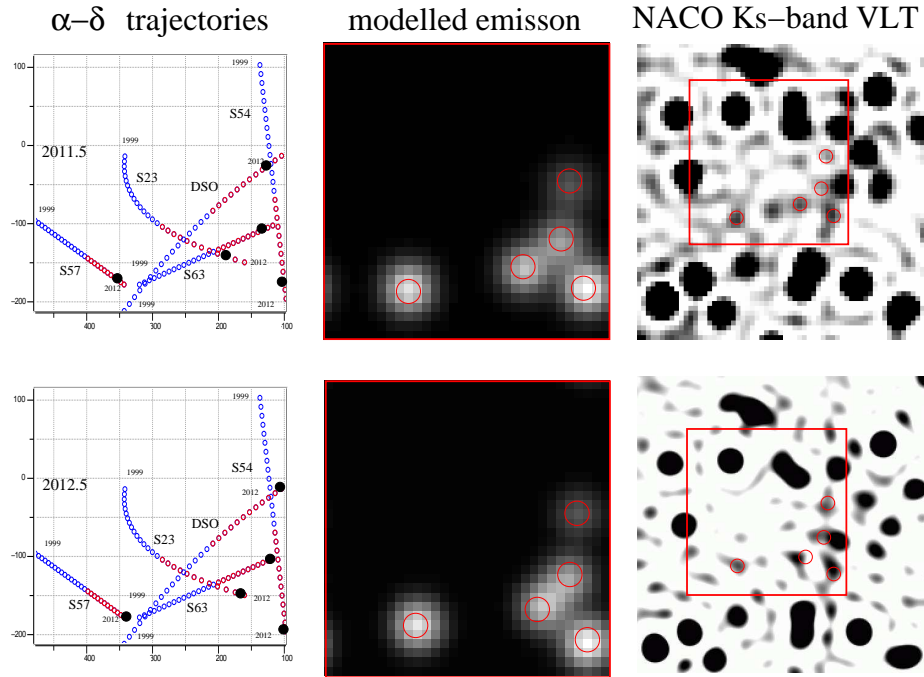


Figure 6: K_s -band identification of the DSO for epochs 2011 and 2012 shown with deconvolved NACO data (at ~ 40 mas resolution) and using the improved kinematic model from Tab 2. See caption of Fig.5.

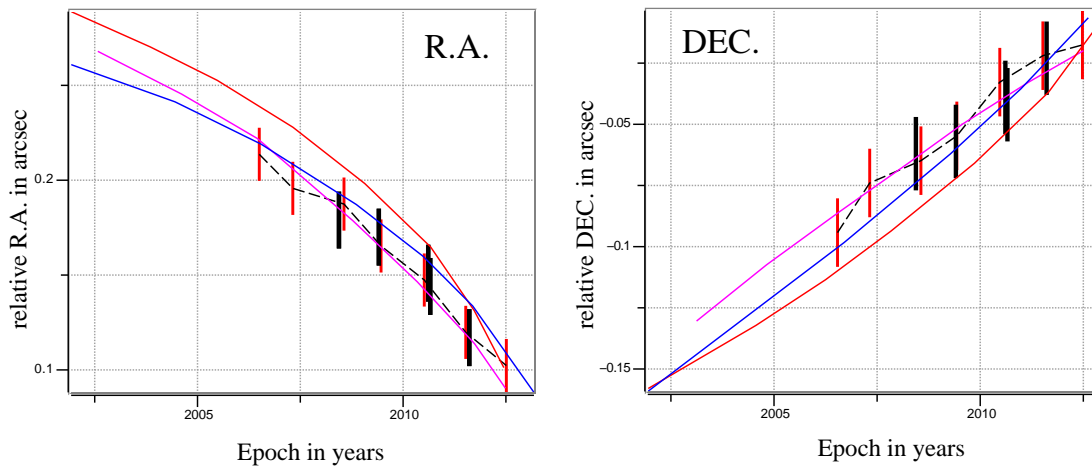


Figure 7: A comparison between the L' -band tracks of the DSO used by Gillessen et al. (2013) (magenta line; L' -band), Phifer et al. (2013) (blue (K' -band $Br\gamma$) and red (L' -band) lines). We also show the coordinates obtained from the K_s -band identification by Eckart et al. (2013) using VLT NACO data (data points with red error bars connected by a black dashed line). Data point with thick black error bars represent the K' -band identification based on Keck NIRC2 data as presented here.

Name	Epoch year	Flux ratio	$\Delta\alpha$ mas	$\Delta\delta$ mas	pm_α mas yr^{-1}	pm_δ mas yr^{-1}	acc_α mas yr^{-2}	acc_δ mas yr^{-2}
S23	2005.47	1.01	307.4	-89.1	12.81	10.17	-1.153	0.225
S57	2007.46	1.24	393.6	-147.4	9.99	6.05	0.000	0.000
S63	2004.00	0.83	245.0	-150.0	15.00	-5.60	0.000	0.000
DSO	2002.00	0.30	295.0	-160.0	16.50	-16.40	-0.160	-0.240
S54	2006.59	1.36	115.4	-60.1	3.05	23.80	0.000	0.000

Table 2: Improved kinematic modeling of the proper motions of the DSO and nearby sources. Epochs, flux ratios, positions, proper motions, and accelerations used to simulate the DSO and the neighboring stars with results shown here in Figs. 5 & 6 and in Figs. A1, A2 & A3 by Eckart et al. (2013). The flux ratios have been calculated with respect to the mean flux derived ($m_K=17.6$) from the K_s -band magnitudes of S23, S54, S57, and S63 as given by Gillessen et al. (1999). They correspond (with an estimated uncertainty of 30%) to the relative fluxes suggested by the modeling presented in the figures listed above. From the quality of the fit in these figures we estimate that the uncertainties are 10 mas for the coordinates, 1 mas yr^{-1} for the proper motions, and 0.1 mas yr^{-2} for the accelerations.

based instruments. The authors find that a superposition of various warm (200 to 500 K) gas phases is required to explain the observations. The densities around 10^4 to 10^5cm^{-3} are derived for these phases. They appear to be too low to self-stabilize the clumps against their high internal turbulence. Since these values clearly fall below the Roche density of $>10^7 \text{cm}^{-3}$ at the position of the CNB, the authors conclude that the bulk of the material in the CNB does not consist of stable structure and must be rather transient. Densities of $\sim 10^7 \text{cm}^{-3}$ are indicated for CNB molecular clumps through interferometric HCN and HCO^+ measurements by Christopher et al. (2005).

2.6 Variability

In a comprehensive statistical approach and using the complete VLT NACO K_s -band data between 2002 and 2010, Witzel et al. (2012) could give a self-consistent statistical description of the NIR variability of SgrA*. Witzel et al. (2012) could not confirm the earlier claimed two states of variability (Dodds-Eden et al. 2011). We find the NIR variability to be a single-state process forming a power-law distribution of the flux density. This distribution even offers an explanation for the claimed X-ray flare that probably occurred 400 years ago (Revnivtsev et al. 2004, Sunyaev & Churazov 1998, Terrier et al. 2010) as an extreme value of our flare statistics without the need for an extraordinary event. However, it cannot be fully excluded that dusty objects, like the DSO/G2, the X3 and X7 sources, or smaller cloudlets (Gillessen 2012, Eckart et al. 2013, Muzic et al. 2010) may be responsible for rare and sporadic off state accretion events. In bright flares - as they are expected if the DSO/G2 leads to an enhanced accretion during or past its SgrA* flyby - QPOs (quasi periodic oscillations) may occur that probe the last stable orbit region of SgrA* and allow to constrain the BH spin (Zamaninasab et al. 2010; Eckart et al. 2006).

These phenomena are observed in nearby galactic nuclei: Temporary QPO features have also been detected in Seyfert 1 nucleus of RE J1034+396 (Middleton, Uttley, & Done 2011). Cenko et al. (2012) report on a short-lived, luminous flare from the nuclear region of a star-forming galaxy

that may be the result of an interaction between a stellar object and a SMBH. The conditions under which these phenomena occur can probably be studied best at the center of the Milky Way.

There are various approaches to physically model and understand the steady state variability of SgrA*. Eckart et al. (2012) use the total NIR/X-ray flux densities and a Synchrotron/Self-Compton model with adiabatic expansion to match the radio. The adiabatic time-lag is measured best with the large frequency separation offered by LABOCA/SABOCA (345 & 850 GHz). The typical adiabatic expansion speeds of $\leq 0.1c$ are too slow for material to leave the immediate vicinity of SgrA*. The expansion must either take place in an orbiting disk or in a jet component with a higher bulk velocity. Larger scales, i.e. separations of $\leq 0.5''$ i.e. within the Bondi sphere - are usually described by magneto-hydrodynamical (MHD) models (Moscibrodzka et al. 2009, Dexter et al. 2010, Shcherbakov & Baganoff 2010). The mid-plane of these models can be described using a 3D relativistic disk code (e.g. Valencia-S., Bursa et al. 2012; capable of investigating the effect of radiative transport and polarization). Indications for a 3 pc scale jet recently outlined by Yusef-Zadeh et al. (2012) are in agreement with the overall orientation of the SMBH and the corresponding spin-axis as derived by Zamaninasab et al. (2011).

3. Conclusion

Based on the work of Contini (2011) and Ho (2008), the Galactic Center can be regarded as a LLAGN in a faint or even off-state. Based on recent work in the radio, infrared and X-ray regime, the center of the Milky Way has all the necessary building blocks that may be required for a bona fide LLAGN. The analysis of the central stellar cluster indicates the presence of young stars (e.g. Buchholz et al. 2009, Schödel et al. 2009, 2010; see also Arches and Quintuplet clusters). Both the NACO VLT and NIRC2 Keck data support the identification of the DSO/G2 with a $2\mu\text{m}$ continuum source. This suggests that we see photospheric emission from dusty star (details in Eckart et al. 2013). The uncertainties between the K- and L'-band measurements obtained by the VLT and Keck suggest that the orbit of the DSO is currently not well defined. Dusty sources that may be linked to young and recently formed stars are also present in the central stellar cluster (Eckart et al. 2013 and references there in). Combined with the sub-mm observations that reveal dusty molecular cloud complexes, this shows that there is the potential for ongoing star formation in the LLAGN at the center of the Milky Way. There are three main points that can be concluded: i) There is an indication that the overall efficiency for accretion events in LLAGN is low (Ho 2008) which is consistent with the SgrA* NIR variability statistics that can explain the X-ray flare about 400 years ago (Witzel et al. 2012); ii) There is an observational indication of an accretion wind associated with the SMBH SgrA* (e.g. Muzic et al. 2007, 2010, Zamaninasab 2011); iii) Sporadic accretion events can be expected in the near future due to the DSO flyby (Gillissen et al. 2012, Eckart et al. 2013). This scenario supports the assumption that the Milky Way may in fact harbor a LLAGN at its center.

Acknowledgements: This work was supported in part by the Deutsche Forschungsgemeinschaft (DFG) via the Cologne Bonn Graduate School (BCGS), and via grant SFB 956, as well as by the Max Planck Society and the University of Cologne through the International Max Planck Research School (IMPRS) for Astronomy and Astrophysics. This research has made use of the Keck Observatory Archive (KOA), which is operated by the W. M. Keck Observatory and the NASA Exoplanet Science Institute (NExSci), under contract with the National Aeronautics and Space Administration. The datasets used have the following PIs: J.Lu, M.R.Morris & T.Soifer. We had fruitful discussions with members of the European Union funded

COST Action MP0905: Black Holes in a violent Universe and the COST Action MP1104: Polarization as a tool to study the Solar System and beyond. We received funding from the European Union Seventh Framework Programme (FP7/2007-2013) under grant agreement No.312789.

References

- [1] Beifiori, A.; Courteau, S.; Corsini, E. M.; Zhu, Y., 2012, MNRAS 419, 2497
- [2] Burkert et al. 2012, ApJ 750, 58
- [3] Bertram, T.; Eckart, A.; Fischer, S.; Zuther, J.; et al., 2007, A&A 470, 571
- [4] Bremer, M.; Scharwächter, J.; Eckart, A.; Zuther, J.; et al., 2012, JPhCS 372, 2054
- [5] Buchholz, R.M.; Witzel, G.; Schödel, R.; et al., 2011, A&A 534, 117
- [6] Buchholz, R.M.; Witzel, G.; Schödel, R., A. Eckart; 2013, A&A 557, 82
- [7] Casasola, V.; Hunt, L. K.; Combes, F.; Garcia-Burillo, S.; et al., 2010, A&A 510, 52
- [8] Casasola, V.; Garcia-Burillo, S.; Combes, F.; et al., 2011, MSAIS 18, 43
- [9] Cenko, S.B.; Bloom, J.S.; Kulkarni, S.R.; et al., 2012, MNRAS 420, 2684
- [10] Contini, M., 2011, MNRAS 418, 1935
- [11] Christopher, M.H.; Scoville, N.Z.; Stolovy, S.R.; Yun, Min S. 2005, ApJ 622, 346
- [12] Dexter, J., Agol, E., Fragile, P. C., McKinney, J. C., 2010, ApJ 717, 2, 1092
- [13] Do, T.; Lu, J. R.; Ghez, A. M.; et al., 2013, ApJ 764, 154
- [14] Do, T., Ghez, A. M., Morris, M. R., et al. 2009, ApJ, 703, 1323
- [15] Dodds-Eden et al. 2011, ApJ 728, 37
- [16] Eisenhauer, F.; Genzel, R.; Alexander, T., et al., 2005, ApJ 628, 246
- [17] Eckart, A.; Muzic, K.; Yazici, S.; Sabha, N.; Shahzamanian, B.; Witzel, G.; Moser, L.; Garcia-Marin, M.; Valencia-S., M.; Jalali, B.; and 6 coauthors 2013, A&A 551, 18
- [18] Eckart, A., Garcia-Main, M.; Vogel, S., N. et al. 2012, A&A 537, 52
- [19] Eckart, A.; Schödel, R., Garcia-Main, M., et al. 2008, A&A 492, 337
- [20] Eckart, A., Eckart, A.; Schödel, R.; Meyer, L.; et al. 2006, A&A 455, 1
- [21] Eckart, A.; Moutaka, J.; Viehmann, T.; Straubmeier, C.; Mouawad, N., 2004, ApJ 602, 760
- [22] Eckart, A.; Genzel, R., 1997, MNRAS 284, 576
- [23] Eckart, A.; Genzel, R., 1996, Nature 383, 415
- [24] Eckart, A.; Genzel, R.; Ott, T.; Schödel, R., 2002, MNRAS 331, 917
- [25] Fischer, S.; Smajic, S.; Valencia-S, M.; Vitale, A.; Zuther, J.; Eckart, A., 2012, JPhCS 372, 2057
- [26] Fisher, D.B.; Bolatto, A.; et al., 2013, ApJ 764, 174
- [27] Garcia-Burillo, S.; Combes, F., 2012, JPhCS 372, 2050

- [28] Garcia-Burillo, S.; Combes, F.; Usero, A.; Gracia-Carpio, J., 2008, JPhCS 131, 2031
- [29] Garcia-Marin, M.; Eckart, A.; Weiss, A. 2011, ApJ 738, 158
- [30] Ghez, A. M.; Duchêne, G.; Matthews, K.; Hornstein, S. D.; et al., 2003, ApJ 586, L127
- [31] Gillessen et al. 2012, Nature.481, 51
- [32] Gillessen et al. 2013, ApJ 763, 78
- [33] Gillessen, S.; Eisenhauer, F.; Fritz, T. K., et al., 2009, ApJ 707, 114
- [34] Ho, L.C., 2008, ARAA 46, 475
- [35] Krips, M.; Martin, S.; Eckart, A.; et al., 2011, ApJ 736, 37
- [36] Laor, A., 2003, ApJ 590, 86
- [37] Levin, Y., & Beloborodov, A. M. 2003, ApJL, 590, L33
- [38] Maoz, Dan, 2008, JPhCS 131, 2036
- [39] Middleton, M.; Uttley, P.; Done, C., 2011, MNRAS 417, 250
- [40] Moscibrodzka, M., Gammie, C. F., Dolence, J. C., et al., 2009, ApJ 706, 1, 497
- [41] Moultaqa, J.; Eckart, A.; Viehmann, T., 2004, A&A 425, 529
- [42] Moultaqa, J.; Eckart, A.; Schödel, R. 2009, ApJ 703, 163
- [43] Muzic, K., Eckart, A.; Schödel, R.; et al. 2010, A&A 521, 13
- [44] Muzic, K.; Schödel, R.; Eckart, A.; Meyer, L.; Zensus, A., 2008, A&A 482, 173
- [45] Muzic, K.; Eckart, A.; Schödel, R.; Meyer, L.; Zensus, A., 2007, A&A 469, 993
- [46] Nicastrò, F., 2000, ApJ 530, L65
- [47] Phifer, K.; Do, T.; Meyer, L.; Ghez, A. M.; Witzel, G.; Yelda, S.; Boehle, A.; Lu, J. R.; Morris, M. R.; Becklin, E. E.; Matthews, K., 2013, ApJ 773, L13
- [48] Shcherbakov, R.V.; Baganoff, F.K., 2010, ApJ 716, 504
- [49] Rauch, C., Muzic, K., Eckart, A., et al., 2013, A&A 551, 35
- [50] Requena-Torres, M. A.; Güsten, R.; et al., 2012, A&A 542, L21
- [51] Revnivtsev, M. G., Churazov, E. M., Sazonov, S. Y., et al. 2004, A&A, 425, L49
- [52] Sunyaev, R. & Churazov, E. 1998, MNRAS, 297, 1279
- [53] Sabha, N.; Eckart, A.; Merritt, D.; Zamaninasab, M, 2012, A&A 545, 70
- [54] Scharwächter, J.; Dopita, M. A.; Zuther, J.; et al., 2011, AJ 142, 43
- [55] Schödel, R. Najarro F. Muzic, K.; Eckart, A., 2010 A&A 511, 18
- [56] Schödel, R.; Merritt, D.; Eckart, A. 2009, A&A 502, 91
- [57] Schödel, R.; Ott, T.; Genzel, R.; Eckart, A.; Mouawad, N.; Alexander, T., 2003, ApJ 596, 1015
- [58] Schödel, R.; Ott, T.; et al., 2002, Nature 419, 694
- [59] Schödel, R.; Merritt, D.; Eckart, A., 2009, A&A 502, 91
- [60] Shcherbakov & Baganoff, 2010 ApJ716, 504

- [61] Smajić, S.; Fischer, S.; Zuther, J.; Eckart, A., 2012, *A&A* 544, 105
- [62] Stolovy, S.R.; Hayward, T.L.; Herter, T., 1996, *ApJ* 470, L45
- [63] Terrier, R., Ponti, G., Belanger, G., et al. 2010, *ApJ*, 719, 143
- [64] Valencia-S., M.; Zuther, J.; Eckart, A.; Garcia-Marin, M.; et al.. 2012, *A&A* 544, 129
- [65] Valencia-S., M., Bursa, M., et al. 2012, *JPhCS.372a2073V*
- [66] Vitale, M.; Zuther, J.; Garcia-Marin, M.; Eckart, A.; et al., 2012, *A&A* 546, 17
- [67] Viehmann, T., et al. 2005, *A&A* 433, 117
- [68] Viehmann, T., et al. 2006, *A&A* 642, 861
- [69] Vollmer, B.; Duschl, W.J., 2000, *NewA* 4, 581
- [70] Witzel, G.; Eckart, A.; Buchholz, R. M.; 2011, *A&A* 525, 130
- [71] Witzel, G.; Eckart, A.; Bremer, M.; et al. 2012, *ApJS* 203, 18
- [72] Xu, Y.; Cao, X.-W., 2007, *ChJAA* 7, 63
- [73] Yusef-Zadeh, F.; Arendt, R.; Bushouse, H.; et al., 2012, *ApJ* 758, L11
- [74] Zamaninasab, M.; Eckart, A.; Witzel, G.; et al. 2010, *A&A* 510, 3
- [75] Zamaninasab, M.; Eckart, A.; Dovciak, M.; et al. 2011, *MNRAS* 413, 322
- [76] Zhao, J.-H.; Morris, M.R.; Goss, W.M.; An, T., 2009, *ApJ* 699, 186
- [77] Zuther, J.; Fischer, S.; Eckart, A., 2008, *JPhCS*, 131, 2042
- [78] Zuther, J.; Fischer, S.; Eckart, A., 2012, *A&A* 543, 57